PHYSICAL REVIEW B, VOLUME 63, 094401

Triplet dispersion in $CuGeO_3$: Perturbative analysis

Christian Knetter* and Götz S. Uhrig†
Institut für Theoretische Physik, Universität zu Köln, Zülpicher Strasse 77, D-50937 Köln, Germany

(Received 13 April 2000; revised manuscript received 31 August 2000; published 25 January 2001)

We reconsider the two-dimensional model for $CuGeO_3$ introduced previously [Phys. Rev. Lett. **79**, 163 (1997)]. Using a computer aided perturbation method based on flow equations we expand the 1-triplet dispersion up to 10th order. The expansion is provided as a polynom in the model parameters. The latter are fixed by fitting the theoretical result to experimental data obtained by inelastic neutron scattering. For a dimerization $\delta \approx 0.08(1)$ we find an excellent agreement with experiment. This value is at least 2 to 3 times higher than values deduced previously from one-dimensional chain approaches. For the intrachain frustration α_0 we find a smaller value of 0.25(3). The existence of interchain frustration conjectured previously is confirmed by the analysis of temperature-dependent susceptibility.

DOI: 10.1103/PhysRevB.63.094401 PACS number(s): 75.40.Gb, 75.10.Jm, 75.50.Ee

I. INTRODUCTION

The dispersion of the magnetic excitations is an important source of information on experimental low-dimensional spin systems. Knowledge of the dispersion relation $\omega(\vec{k})$ helps essentially to identify the model appropriate to describe the compound under study. The dispersion relation provides also important insight in the nature of the ground state. Very common in low-dimensional systems is the scenario of a singlet $S=0$ ground state *without* magnetic long-range order (a ''spin liquid'') of which the elementary excitations are triplets $S=1$. These systems are generically gapped. Examples are isolated or weakly coupled dimerized spin chains and spin ladders such as $(VO)_2P_2O_7$,[1] the spin-Peierls phase of $CuGeO_3$,[2,3] and $SrCu_2O_3$.[4] A true two-dimensional (2D) example is $SrCu_2(BO)_2$ which is characterized by frustrated dimers.[5–7]

In these gapped $S=1/2$ systems where the gap is related to some ''strong'' bond (which can be also the rung of a two-leg ladder) the elementary triplet excitations are in principle accessible by a perturbative expansion about the limit of isolated dimers. This approach, however, becomes tedious for the description of realistic materials since the expansion parameter is often not really small. Thus one has to compute high orders to achieve quantitative agreement. For this reason various automated approaches have been conceived which leave the tedious part to computers.[8–11]

In the present article, we will apply the previously introduced perturbation by flow equation[11] to the two-dimensional, though anisotropic, system of $CuGeO_3$ in its dimerized low-temperature phase.[2] Thereby we extend the previous analysis (Ref. 3, henceforth cited as I) considerably. Our starting point remains the same as before. The strongest coupling is given by J; the other couplings are given relative to J as indicated in Fig. 1 (for details see Fig. 1 in I).

Our work has two objectives. One is to show that the perturbation method introduced previously[11] can be also applied to two-dimensional systems. The other is to determine within the framework of a static spin model the microscopic parameters for $CuGeO_3$.

II. METHOD

The problem to be solved reads

$$H=H_0+\lambda H_S, \tag{1}$$

where H_0 and H_S are schematically given by (see lines in Fig. 1).

$$H_0/J=\sum S \;\rule[0.5ex]{2em}{2pt}\; S$$

$$H_S/J=\sum S \;\rule[0.5ex]{2em}{0.4pt}\; S+\alpha\sum S \;\rule[0.5ex]{2em}{0.4pt}\; S$$

$$+\frac{\mu}{\lambda}\sum S\text{---}S+\frac{\mu\beta}{\lambda}\sum S-\cdot\cdot-S.$$

As in the chain in Ref. 11 the isolated dimer limit ($\lambda=0$ at finite μ/λ) has an equidistant energy spectrum and the perturbation can alter the number of energy quanta (here: triplets on the dimers) by 2 at maximum. Hence H_S can be represented as $H_S=T_{-2}+T_{-1}+T_0+T_1+T_2$, where T_i stands for the perturbing part changing the number of elementary triplets by i. The same formalism as in Ref. 11 can be used. This formalism maps the perturbed Hamiltonian by a continuous unitary transformation, the so-called flow equation method,[12] to an effective Hamiltonian H_{eff} which *conserves* the number of energy quanta, i.e., $0=[H_{\text{eff}},H_0]$. The effective Hamiltonian has the form

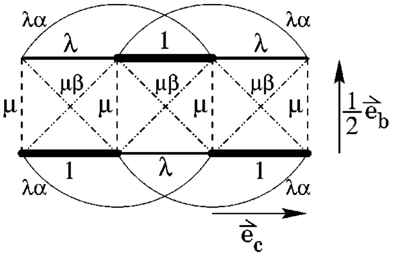

FIG. 1. Dimerization pattern in the dimerized low-temperature phase of $CuGeO_3$. The couplings are denoted relative to the strongest coupling J which is set to unity in the figure.

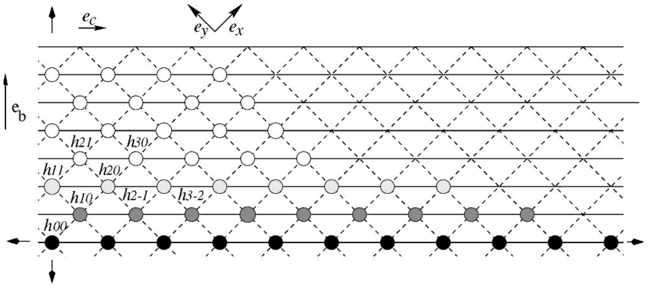

FIG. 2. Effective lattice on which the triplet hops. We calculate the amplitudes $h_{j,l}$ for all hopping processes starting on (0,0) and ending on one of the depicted dimers (circles). For all circles that are accessible by an arbitrary hopping length of 6 or less the amplitudes have been calculated within 6th order. (The length of a hop is the minimum number of bonds (solid or dashed) required to link the start and end point.) The amplitudes for light gray, dark gray, and black circles have been extended in 8th order, provided that these sites can be reached by a hopping $\propto \mu^2$ of length 8. Analogously, the amplitudes for dark gray and black circles were extended by calculating hopping processes $\propto \mu^1$ within 9th order. Finally, the amplitudes for all black circles were extended by processes $\propto \mu^0$ within 10th order. The arrows indicate axes with respect to which reflection symmetry holds.

$$H_{\text{eff}} = H_0 + \sum_{k=1}^{\infty} \lambda^k \sum_{|\underline{m}|=k, M(\underline{m})=0} C(\underline{m}) T(\underline{m}), \tag{2}$$

where $\underline{m} = (m_1, m_2, \ldots m_k)$ is a vector of dimension $|\underline{m}| = k$ of which the components m_i are in $\{\pm 2, \pm 1, 0\}$; $M(\underline{m}) = \Sigma_{i=1}^{k} m_i = 0$ signifies that the sum of the components vanishes which reflects the conservation of the number of energy quanta (triplets). In each order k one has to evaluate the restricted sum over the operator products $T(\underline{m}) = T_{m_1} T_{m_2} \cdots T_{m_k}$. The coefficients $C(\underline{m})$ are generally valid fractions computed up to order $k = 10$ in Ref. 11 where also further details on the flow equation method can be found. The products $C(\underline{m}) T(\underline{m})$ can be viewed as weighted virtual processes.

Since H_{eff} conserves the triplet number the one-triplet sector is particularly easy to solve. Acting on one triplet the action of H_{eff} may only consist in shifting the triplet. This means that the triplet hops on an effective lattice where one site stands for one dimer on the original lattice (see Fig. 2 in I or Fig. 2).

The full dispersion $\omega(\vec{k})$ is obtained by Fourier transform

$$\omega(\vec{k}) = J \sum_{j,n} h_{j,n} \exp[i(k_1 j + k_2 n)]. \tag{3}$$

The hopping amplitudes $h_{j,n}$ can be calculated on finite clusters of the (in principle infinite) effective lattice: From the linked cluster theorem we know that the finite order contribution of a short-ranged perturbation does not depend on the cluster size for sufficient large clusters. Carrying out our perturbation within order l implies that one allows dimer to dimer hopping processes of length l.[11] The minimum cluster for a given amplitude $h_{j,n}$ in a given order l contains all dimers and links that are involved in a hopping of length $\leqslant l$ starting at dimer (0,0) and ending at (j,n). The minimum cluster is determined by considering all paths from (0,0) to (j,n). All dimers and links covered by one of these paths are part of the minimum cluster. In Fig. 3, the computer generated minimum cluster for calculating $h_{3,-1}$ in order 8 is shown.

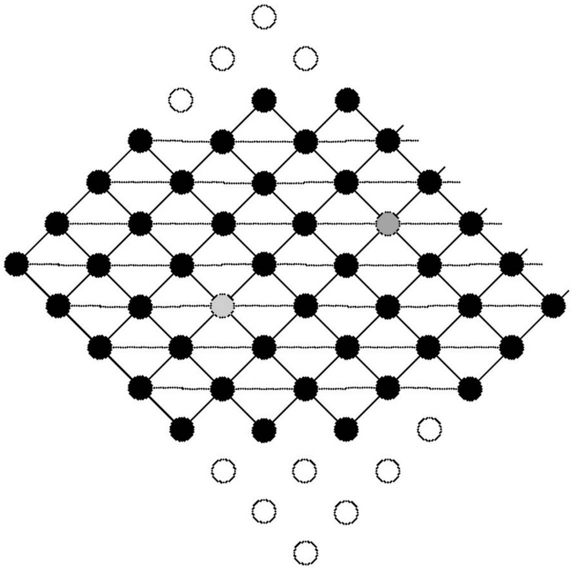

FIG. 3. Computer generated cluster necessary to compute $h_{3,-1}$ in 8th order, allowing for arbitrary hopping processes of length 8. The light gray (dark gray) circle denotes the start (end) dimer $(0,0)(3,-1)$.

Due to the strong anisotropy of the quasi-1D system CuGeO_3 it is reasonable to use higher-order terms only along the chains. This simplifies the computational task considerably since the calculation of a hopping process along the chain is much simpler. The cluster to be considered can be chosen smaller. The same is true for hopping processes *close* to the chain direction. Here we restrict the hopping processes to be at maximum quadratic in the interchain hopping μ, which reduces the cluster sizes significantly so that the perturbation order can be enlarged.

III. ANALYSIS OF EXPERIMENTAL DATA

The results for the $h_{j,n}$ are too lengthy to be published in written form. We will provide them in electronic form on our home pages on appearance of this article. In I the $h_{j,n}$ in third order in λ and μ were presented. A few of these are erroneous. They are corrected herewith.[13] The corrections, however, have no influence on the conclusions in I (see also discussion below).

Once all amplitudes $h_{j,n}$ are calculated the dispersion relation is given by Eq. (3). After rewriting Eq. (3) in terms of k_b and k_c (the reciprocal basis to e_b and e_c) we add the term $4t_a \cos(k_a)\cos(k_c)$ with $4t_a = 0.22$ meV to account for the dispersion in a direction (cf. I). To fix the parameters J, α, β, μ and λ (cf. Fig. 1) we use the one-magnon dispersion data for CuGeO_3 experimentally determined by inelastic neutron scattering.[14] Note that the hopping amplitudes are computed as polynomials over $\mathbb{Q}$ in the parameters.

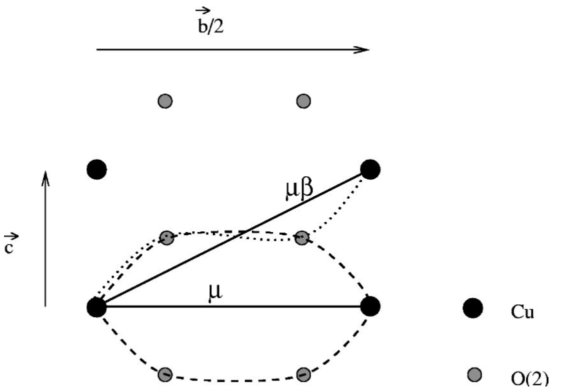

FIG. 4. Schematic view of the microscopic super-exchange paths between the chains (running along the c direction) in CuGeO$_3$. The three-dimensional situation is depicted in Ref. 16.

As noticed in I the parameter β has almost no influence on the shape of the dispersion. Hence we refrain from determining β from the dispersion but set it beforehand to some reasonable values in the interval $[-0.3,0.3]$. This choice is motivated by comparing the microscopic *direct* super-exchange path μ and the *shifted* super-exchange path $\mu\beta$ shown schematically in Fig. 4 (cf. Fig. 1). There is only one path per Cu^{2+}-site for the shifted coupling whereas there are two paths for the direct coupling. Thus we expect $|\mu\beta| \approx 1/2|\mu|$, i.e., $|\beta| \approx 0.5$. There are also results from *ab initio* calculation for the interchain couplings which indicate the existence of interchain frustration.[15] Further evidence is provided below by the analysis of the susceptibility. Furthermore, we find that for $|\beta| > 0.4$ fits to the dispersion data become worse.

To determine the remaining parameters we equate four different experimental points with the corresponding parameter dependent dispersion values given by Eq. (3). The experimental points were chosen such that the maxima of the dispersion (two points) and the high-precision data points at $k_c < 0.1$ are fitted as good as possible. In Figs. 5 and 6 they are indicated by arrows. This approach was chosen to illustrate explicitly how delicately the dispersion shape, in particular the curvature at the minimum, depends on the frustration. The parameters are fixed by solving the resulting system of equations. For $\beta = 0.3$ and -0.3 Figs. 5 and 6 show the resulting dispersion curves in c* and in b* direction, respectively, using all $h_{j,n}$ calculated.

As can be seen from Figs. 5 and 6 the plain series up to 10th order provides excellent fits. Yet one realizes that the parameter values still change on passing from order to order. So it appears that even at 10th order the results are not quantitative. In order to obtain quantitative reliable results we adopt a systematic extrapolation in the order. In each order $l \in \{3,4, \ldots 10\}$ we determine the optimum fit parameters. For illustration, Fig. 7 shows results for $\beta = 0.3$.

Assuming exponential convergence we use

$$f(l) = X - be^{-2cl}, \tag{4}$$

where X is the asymptotic value of the parameter considered and b and c are constants. The choice (4) is motivated on one hand by its obvious applicability (see Fig. 7). On the other it stems from the fact that CuGeO$_3$ is a quasi-one-dimensional gapped spin system. So one expects the magnetic correlations to drop exponentially with distance. Furthermore the order l determines the maximum distance over which correlations occur (cf. Ref. 11), namely l counted in dimers or $2l$ counted in spin sites. Hence the constant c in Eq. (4) can be understood as the inverse of a correlation length ξ. With the usual relation $\xi \approx v_S/\Delta$ for one-dimensional systems we obtain $c \approx 1/6$ based on the rough estimates $v_S = \pi/2 \cdot J(1 - 1.12\alpha_0)$ (Ref. 17) and $\alpha_0 \approx 0.3; J \approx 12$ meV$; \Delta \approx 2$ meV. This is indeed what is found (cf. Tables I and II) so that we judge our extrapolations as being well justified.

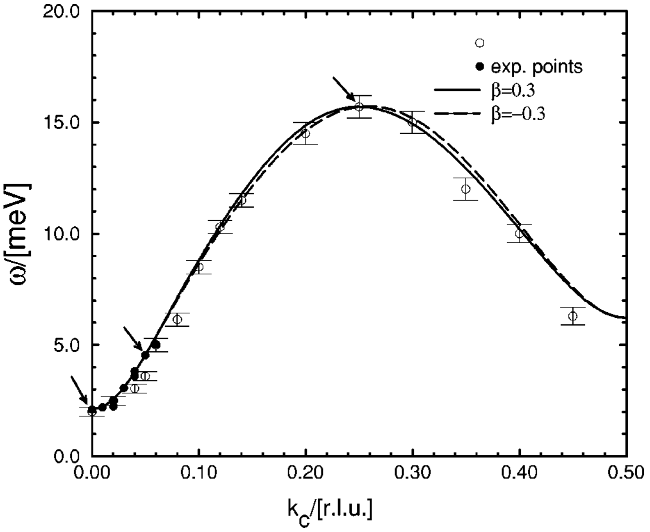

FIG. 5. Dispersion $\omega(k_a=0,k_b=0,1/2+k_c)$ in c* direction. The arrows indicate the experimental points used to fix the parameters. 10th order fits based on $(\beta,\lambda,\alpha,\mu,J) = (0.3,\ 0.836,\ 0.225,\ 0.266,\ 13.1\ \text{meV})$ and $(-0.3,\ 0.846,\ 0.209,\ 0.081,\ 12.3\ \text{meV})$, respectively.

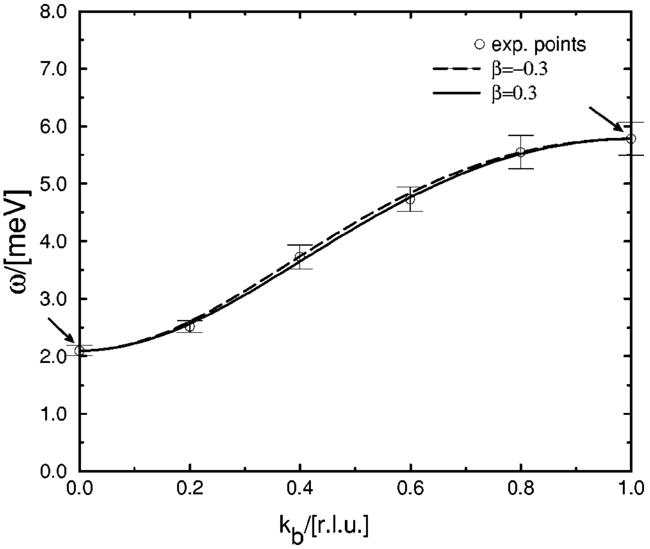

FIG. 6. Dispersion $\omega(k_a=0,k_b,k_c=0)$ in b* direction. Otherwise as in Fig. 5.

TABLE I. Extrapolated parameter values X according to Eq. (4). The experimental points we used in the fit process for this table are (cf. Figs. 5 and 6) $[(k_b,k_c);\omega(\mathbf{k})/\mathrm{meV}]$: [(0,0);2.1], [(0,0.05);4.55], [(0,0.25);15.7], [(1,0);5.78].

	All points considered			last four points considered		
	X	b	c	X	b	c
			$\beta=0.3$			
α	0.245	2.61	0.249	0.236	8.24	0.338
λ	0.867	0.501	0.155	0.840	8.66	0.418
J/meV	13.6	11.0	0.164	13.2	105	0.357
			$\beta=0.22$			
α	0.232	3.27	0.268	0.228	9.50	0.343
λ	0.863	0.681	0.184	0.842	13.6	0.444
J/meV	13.1	11.3	0.171	12.8	68.9	0.324
			$\beta=0$			
α	0.218	4.16	0.294	0.226	9.20	0.334
λ	0.862	0.902	0.213	0.848	14.94	0.442
J/meV	12.8	11.1	0.174	12.6	44.48	0.287
			$\beta=-0.3$			
α	0.212	4.48	0.300	0.222	9.94	0.337
λ	0.863	0.974	0.218	0.849	16.5	0.448
J/meV	12.7	10.9	0.173	12.5	42.2	0.282

In Fig. 7 the extrapolations are depicted by lines. The solid lines were obtained by using all calculated parameter values. The dashed lines are obtained from on the last four points, i.e., the results in order 7, 8, 9, and 10. The deviation between these two extrapolations are used as a measure for the extrapolation error. This procedure is carried out for α, λ, and J.

There is no systematic dependence of μ on the order l. The parameter μ fluctuates between the two thin horizontal lines in Fig. 7. From this we conclude that the dependence of μ on the order is fairly small though not negligible. The size of the fluctuation determines the reliability of the approximation of working with truncated series. So we take the average of the two bounds as our estimate for μ and their difference as the error in the determination of μ.

Tables I and II summarize the results of the fits for the parameters α, λ, and J for four preset values of β. The values for μ are listed in Table III.

TABLE II. Same as in Table I based on different experimental points: [(0,0);2.1], [(0,0.05);4.35], [(0,0.25);15.7],[(1,0);5.78].

	All points considered			last four points considered		
	X	b	c	X	b	c
			$\beta=0.3$			
α	0.297	1.41	0.215	0.309	1.18	0.187
λ	0.868	0.423	0.197	0.877	0.404	0.165
J/meV	14.3	8.88	0.142	13.9	37.4	0.269
			$\beta=0.22$			
α	0.301	1.41	0.208	0.318	1.15	0.175
λ	0.867	0.850	0.274	0.886	0.526	0.175
J/meV	13.6	12.0	0.191	13.8	15.2	0.191
			$\beta=0$			
α	0.308	1.34	0.191	0.323	1.30	0.173
λ	0.900	0.38	0.140	0.896	0.754	0.191
J/meV	13.6	8.00	0.133	13.7	9.31	0.139
			$\beta=-0.3$			
α	0.314	1.28	0.180	0.326	1.37	0.173
λ	0.913	0.369	0.127	0.903	0.832	0.192
J/meV	13.6	7.69	0.127	13.6	9.12	0.136

TABLE III. Final parameter intervals resulting from Tables I and II for three different values of β.

parameter	interval	parameter	interval
	$\beta=0.3$		
α	0.27(4)	α_0	0.25(3)
λ	0.86(2)	δ	0.08(1)
μ	0.27(1)	μ_0	0.29(1)
J/meV	13.8(5)	J_0/meV	12.8(6)
	$\beta=0.22$		
α	0.27(4)	α_0	0.25(3)
λ	0.86(2)	δ	0.08(1)
μ	0.21(1)	μ_0	0.23(1)
J/meV	13.4(4)	J_0/meV	12.5(5)
	$\beta=0.0$		
α	0.27(5)	α_0	0.25(5)
λ	0.88(3)	δ	0.07(2)
μ	0.13(1)	μ_0	0.14(1)
J/meV	13.2(6)	J_0/meV	12.4(7)
	$\beta=-0.3$		
α	0.27(5)	α_0	0.25(5)
λ	0.88(3)	δ	0.06(2)
μ	0.08(2)	μ_0	0.09(1)
J/meV	13.1(5)	J_0/meV	12.3(7)

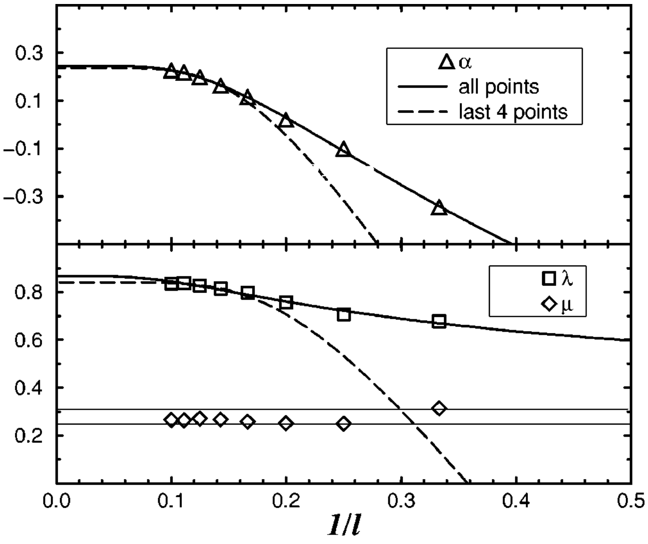

FIG. 7. Dependence of the parameter values on the perturbation order l at $\beta=0.3$. The quasiconstant behavior of μ is found for all β values checked. The lines are fits to the data according to Eq. (4). The solid lines consider all points, the dashed ones only the last four points.

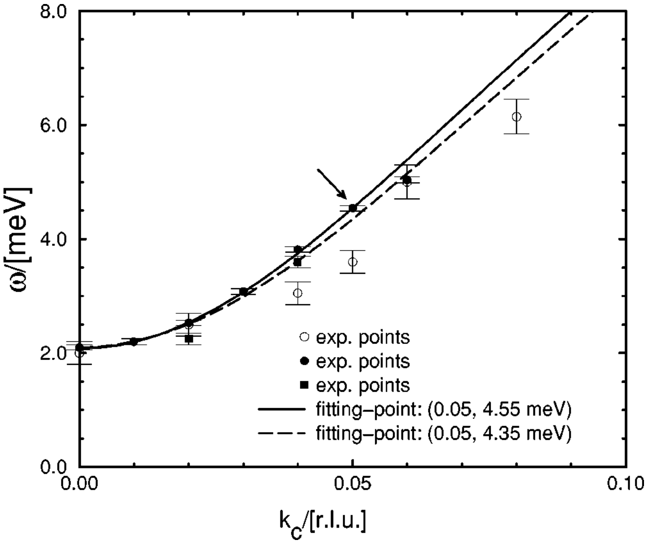

FIG. 8. Enlargement of Fig. 5 for small wave vectors at $\beta = 0.3$. The solid curve is the same as in Fig. 5, leading to Table I. The dashed line corresponds to a 10th order fit where the point ($k_c = 0.05, \omega = 4.55$ meV) indicated by the arrow is replaced by ($k_c = 0.05, \omega = 4.35$ meV), leading to Table II. The filled circles correspond to highly accurate experimental points for which the error bars are of the size of the symbols.

A closer inspection of Figs. 5 and 6 reveals that we are confronted with a certain arbitrariness of which fit we should favor. The experimental errors enhance this problem. The filled circles in the range of small wave vectors in Fig. 5 represent experimental points which have been measured with a high degree of precision. Thus it is reasonable to fit the theoretical curve as well as possible to these points. Figure 8 shows an enlargement of this region. The solid line is the 10th order fit result for $\beta = 0.3$ as the solid line in Fig. 5. The depicted arrow indicates the experimental point ($k_c = 0.05, \omega = 4.55$ meV) used to obtain Table I.

A likewise well suited curve, however, is produced if one uses the point ($k_c = 0.05, \omega = 4.35$ meV) for the fit keeping the other points (Table II). It is not possible to prefer one of the two lines in Fig. 8 to the other on the basis of their agreement to the experimental data. Hence we choose these two fits as the bounds within which all fits are acceptable. The corresponding parameter values X_1 (fit 1) and X_2 (fit 2) provide an interval $[X_1, X_2]$ which we expect to contain the true model parameter $\overline{X}$. Hence the latter is estimated by

$$\overline{X} = (\overline{X}_1 + \overline{X}_2)/2 \pm \Delta\overline{X},$$

with $\overline{X}_i = 1/2(X_i^{\text{all points}} + X_i^{\text{last 4 points}})$, $\Delta\overline{X}_i = |\overline{X}_i - X_i^{\text{all points}}|$, and $\Delta\overline{X} = \max\{|\overline{X} - \overline{X}_1|, \Delta\overline{X}_1, \Delta\overline{X}_2\}$. The results are summarized in Table III.

For the readers' convenience Table III also gives the results in the more commonly used parameters δ, α_0, μ_0, J_0, and β. This notation is connected to the one used so far in this article by

$$J = J_0(1+\delta), \qquad \lambda = \frac{1-\delta}{1+\delta},$$

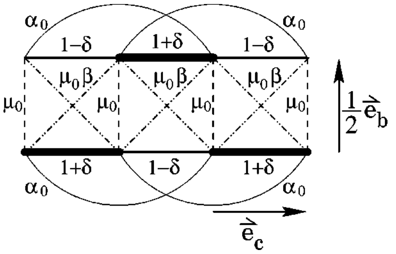

FIG. 9. Alternative notation for the couplings in the dimerized phase of CuGeO$_3$. The couplings are denoted relative to the average nearest-neighbor coupling J_0 in the chains.

$$\alpha = \frac{\alpha_0}{1-\delta}, \qquad \mu = \frac{\mu_0}{1+\delta}. \tag{5}$$

It corresponds to the Hamiltonian depicted in Fig. 9.

IV. IMPLICATIONS FOR THE SUSCEPTIBILITY

The temperature dependence of the homogeneous susceptibility $\chi(T)$ is often used to determine the parameters of CuGeO$_3$.[3,18–21] Already the Curie-Weiss temperature Θ provides valuable information on the sum of the coupling constants. This is particularly useful to detect frustration. The dispersions are governed by the difference of the direct and the frustrating coupling whereas $\chi(T)$ at larger temperatures is more influenced by the sum of direct and frustrating coupling.

The analysis of the Curie-Weiss temperature alone bears some risks. It is easy to calculate but difficult to determine experimentally since it has to be deduced from values at high temperatures where $\chi(T)$ is fairly small and hence strongly influenced by background effects (van Vleck, diamagnetism) or by slight structural changes.

A convincing fit for temperatures above 50 K is given by Fabricius *et al.* in Ref. 20 on the basis of frustrated chains. The inclusion of interchain couplings, however, would spoil the excellent agreement and a redetermination of the constant would be necessary. A description of $\chi(T)$ on the basis of a two-dimensional model has not been done except for a consideration of the two leading coefficients in an expansion in $1/T$ in I. In Fig. 10 we show the same high quality experimental data as in Ref. 20 and compare it to theoretical curves at four values of β with corresponding parameter values J, λ and α as given in Table III. The theoretical curves are obtained by computing a [4,5] Dlog Padé approximant $\chi_0(T)$ based on the high-temperature series provided in Ref. 22 for the frustrated chains. This procedure provides excellent results down to $T \approx J/5$.[23] The asymptotic behavior of the approximant is chosen such that $\chi_0(T)$ vanishes linearly on $T \to 0$ as is to be expected for a two-dimensional massless antiferromagnet. Besides this feature the two dimensionality is incorporated on a chain-mean-field level

$$\chi(T) = \frac{\chi_0(T)}{1 + 2\mu_0(1+2\beta)\chi_0(T)}. \tag{6}$$

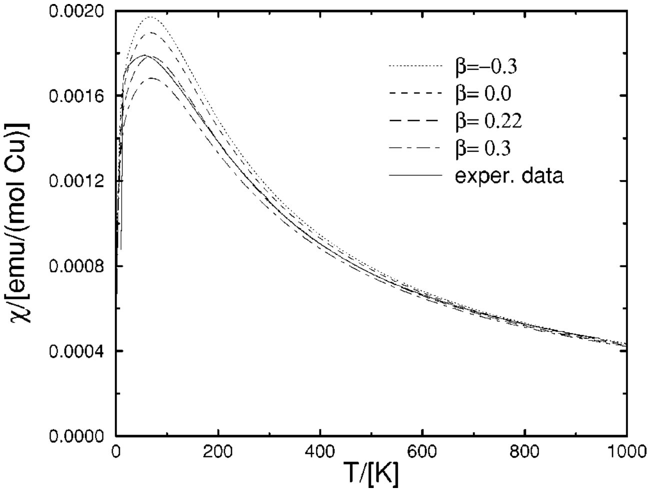

FIG. 10. Comparison of experimental data in b direction (Ref. 20) and theoretical susceptibilities for various values of the interchain frustration. The g value used is 2.26 (Refs. 24 and 25).

This relation is exact in linear order in μ. Estimates of corrections quadratic in μ indicate that they are negligible for the values of μ and β in which we are interested.

From the results in Fig. 10 it is evident that the interchain frustration cannot be neglected. Only for a finite value of about 0.22 a very good agreement can be obtained. The agreement to the frustrated chain model[20] is still better since the position of the maximum is also reproduced. But on the basis of the neutron-scattering results[14] it is undoubtful that CuGeO_3 is a two-dimensional substance. Furthermore, it must be considered that the previous fit[20] was a two-parameter (J and α_0) fit whereas only one parameter (β) is fitted to obtain Fig. 10. The other parameters (J_0, α_0, μ_0) were determined from an entirely different experiment. Hence the agreement for $\chi(T)$ corroborates also the validity of the parameters determined in the preceding section.

We want to emphasize that we try to explain simultaneously a $T=0$ and a $T>0$ experiment in the framework of a static model (except for changes in δ). Naturally, fitting the magnetic susceptibility alone (as done in Refs. 18–20) produces better agreement to the experiment.

V. DISCUSSION

We will first discuss our results and propose a set of parameters. Then we will put these results into the context of other results in the literature.

Let us consider the remaining difference between experiment and theory concerning $\chi(T)$ in Fig. 10. There are four conceivable sources for it. The first are experimental inaccuracies. We are not in the position to judge this aspect. We would just like to comment that from the results and error bars in Fig. 8 it is obvious that the experimental data is not completely consistent so that this explanation is possible.

Second, it is conceivable that the couplings change across the transition, i.e., the intrachain frustration at $T\approx 0$ (where the dispersions are measured) is different from the one above T_{SP} [where $\chi(T)$ is measured]. Since we are considering a spin-Peierls transition there is definitely a structural change. So far, however, the assumption that only the dimerization changes worked well. The structural changes in the transition are very small[16] whereas the changes needed to explain the discrepancy are of the order of 20 to 30 % (assuming a change in the intrachain frustration). Estimates point into the direction that the changes on the couplings are unimportant.[26] Yet the estimates concern in the first place the nearest-neighbor coupling only. Quantitative ab initio calculations of the frustration are very difficult,[15] even more so for changes of the frustration. So, again, this explanation is perhaps not the most promising but cannot be excluded either.

Third, the influence of the phonon dynamics is to be considered. It is shown that spin-Peierls systems can be unitarily transformed in such a way that an effective spin model remains at low energies uncoupled to the phonons.[27] The effective couplings in a single chain model become temperature dependent so that this may account for the discrepancy. But it turns out for nonresonant phonons ($\omega>J$) that these effects leave the susceptibility fairly unchanged. This is so since these effects become significant for relatively large temperatures where $\chi(T)$ depends only on the sum of all couplings which is unchanged by the unitary transformation [this is observed in $(\mathrm{VO})_2\mathrm{P}_2\mathrm{O}_7$].[28] So this reason appears rather unlikely even though it looked plausible at first sight.

Fourth, one has to think about any kind of precursors of the spin-Peierls transition. By this we mean on one side the critical fluctuations which appear in a narrow region (≈ 3 K) around the spin-Peierls temperature.[26] On the other side, we mean any precursor which goes beyond a purely static spin model. Experimentally, a finite lattice correlation length can be detected already at $T\approx 40$ K far above the actual transition.[29] From there on deviations from the behavior of a static spin model should be observable. In the adiabatic limit, for instance, the fluctuation yield already a reduction of the susceptibility.[30] What happens in the antiadiabatic limit has not yet been investigated for a two or higher dimensional model. The mapping in Ref. 27 leads to four-point interchain couplings the influence of which is unclear so far.

In view of the above mentioned possible pitfalls of the static model the agreement in Fig. 10 is already very convincing. Summarizing our results we propose the parameters given for $\beta=0.22$ in Table III to be the ones deduced from the dispersion data. Assessing the reliability of our estimates, we redo the analysis of the susceptibility for $\alpha_0=0.28$ (the upper bound of our estimate for α_0) with the corresponding value of $J_0=12.8$ meV. Then the optimum $\chi(T)$ is obtained for $\beta=0.15$; the $\chi(T)$ curve is almost identical to the one shown in Fig. 10. So the value of β cannot be determined very precisely, but it should be in the range $\beta=0.2(1)$. A certain discrepancy between the optimum parameters for the $T=0$ dispersion data and for the $\chi(T>T_{\mathrm{SP}})$ data remains.

We split the comparison of our findings to previous works into three groups. The first comprises the analysis on the basis of a one-dimensional model.[18–20,31] The most striking difference to the results for static spin models[18–20] is that the dimerization δ is not of the order of 1% but significantly larger. This is not astounding since it has been noted already in I that the gap is lowered by the interchain hopping. Hence the neglect of the latter requires to lower the gap otherwise, i.e., by assuming a lower dimerization.

Our intrachain frustration is slightly larger than the one of Castilla *et al*. (0.24), but significantly smaller than the value of Riera and Dobry (0.36) or the value of Fabricius *et al.* (0.35). Fabricius *et al.* showed that the value $\alpha_0 = 0.24$ is too small for a single chain model. The difference between the larger frustration value in the single chain model to our value results directly from the interchain coupling. As can be nicely seen in Eq. (6) the interchain coupling lowers the susceptibility without changing (in the chain mean-field approximation) the position of its maximum. The one-dimensional models favor a larger intrachain frustration and a concomitant larger coupling J in order to reduce the magnitude of the susceptibility.

The claim by Wellein and coworkers that the dimerization, which is experimentally found to be larger than would fit to a static 1D model,[32] is due to the phonon dynamics is not compelling. They use a root-mean-square definition of the dimerization which naturally provides larger values for the dimerization since it includes all the fluctuations. The dispersion perpendicular to the chains, however, is an unambiguous experimental fact. Furthermore, Trebst and coworkers[33] do not find a substantial gap renormalization for parameters relevant for $CuGeO_3$ even though one should take care of different schemes to couple the phonons.

Let us turn to the second group of papers considering the essentially two-dimensional character of $CuGeO_3$. The first work used a bond-operator technique.[34] No frustration was considered, hence rather small values of $J = 10.2$ meV and a rather small interchain hopping $\mu \approx 0.06$ resulted. The same technique was also applied later again by Brenig[35] including frustration. It turned out, however, that only $\lambda(1-2\alpha)$ and $\mu(1-2\beta)$ matter on the free-boson level. Hence an independent determination of the frustration is not possible. Using additional input ($\delta = 0.012$) the values $\alpha_0 = 0.059$ and $\mu(1-2\beta) = 0.054$ were obtained. In view of the extensive comparisons to numerical results made in Ref. 35 it appears that the bond-operator method overestimates the influence of additional couplings such as dimerization or frustration. Generally, the values for dimerization or frustration tend to be too low. This is confirmed by our findings in the present work.

Compared to I ($\alpha_0 = 0$, $J = 9.8$ meV, $\delta = 0.12$, $\mu_0 = 0.34$, $\beta = 0.3$) the extended series on which our present analysis is based gives a much better handle on intrachain frustration, see Fig. 7. Only in the present work, we are able to assess its value reliably. With respect to the interchain frustration, the present results agree qualitatively with those in I where such a frustration was proposed for $CuGeO_3$ first. The use of susceptibility information has been improved in the present work since the whole $\chi(T)$ curve is used, not only the leading coefficients.

Bouzerar *et al.* have carried out an estimate leading to results not too far from ours: $\delta = 0.065$, $\alpha_0 = 0.2$, $J = 12.2$ meV, $\mu = 0.15$. They used just linear order in the interchain hopping without interchain frustration and some square-root averaging with numerical results for chains to describe the dispersion. The intrachain frustration ($\alpha_0 = 0.2$) could only be taken from the Curie-Weiss constant. The resulting $\chi(T)$ has similarities with the experimental one.

The third group comprises ab initio calculations of the exchange couplings and of the spin-phonon couplings. Microscopic calculations[36,16] find relatively large values of the dimerization between 0.07 and 0.2 in agreement with our findings. (Even though there is also a different result.[37]) Very important for our work are recent results by Drechsler and coworkers supporting the existence of interchain frustration.[15] Werner and coworkers[26] estimate a large dimerization from the spin-phonon couplings and the shifts of the ions ($\delta = 0.11$). From the balance of elastic and magnetic energy in the D phase they obtain a lower bound of $\delta > 0.044$ under the assumption of a singlet product ground state. Assuming critical frustration $\alpha_0 = 0.2412$ they find even $\delta > 0.078$ which fits very nicely to our findings.

In summary, we provide by the present work a determination in great detail of the coupling parameters [$\beta = 0.2(1)$ and right column in Table III under $\beta = 0.22$] of $CuGeO_3$ based on a static dimerized spin model at $T = 0$. The experimental input comes from inelastic neutron scattering. The implications of the parameters found for the susceptibility are also studied. Very good agreement could be obtained fitting the interchain frustration appropriately. A small discrepancy at low temperatures around 50 K indicates that the static spin model is probably insufficient to describe $CuGeO_3$ completely. By this work, we proved the outstanding possibilities of high-order series expansions (around the dimer limit or around the limit $T = \infty$) in the analysis of experimental data.

ACKNOWLEDGMENTS

The authors would like to thank B. Büchner, A. Bühler, U. Löw, B. Marić, E. Müller-Hartmann, and F. Schönfeld for fruitful discussions. The provision of the experimental data by B. Büchner, T. Lorenz, and L. P. Regnault is gratefully acknowledged. Furthermore, we thank the Regional Computing Center of the University of Cologne for its kind and efficient support. This work was supported by the Deutsche Forschungsgemeinschaft in the Schwerpunkt 1073 and in the Sonderforschungsbereich 341.

---

*Email address: ck@thp.uni-koeln.de
†Email address: gu@thp.uni-koeln.de

[1] A. W. Garrett, S. E. Nagler, D. A. Tennant, B. C. Sales, and T. Barnes, Phys. Rev. Lett. **79**, 745 (1997).
[2] J. P. Boucher and L. P. Regnault, J. Phys. I **6**, 1939 (1996).
[3] G. S. Uhrig, Phys. Rev. Lett. **79**, 163 (1997).
[4] M. Azuma, Z. Hiroi, M. Takano, K. Ishida, and Y. Kitaoka, Phys. Rev. Lett. **73**, 3463 (1994).
[5] H. Kageyama, K. Yoshimura, R. Stern, N. V. Mushnikov, K. Onizuka, M. Kato, K. Kosuge, C. P. Slichter, T. Goto, and Y. Ueda, Phys. Rev. Lett. **82**, 3168 (1999).
[6] S. Miyahara and K. Ueda, Phys. Rev. Lett. **82**, 3701 (1999).

[7] E. Müller-Hartmann, R. R. P. Singh, C. Knetter, and G. S. Uhrig, Phys. Rev. Lett. **84**, 1808 (2000).

[8] H.-X. He, C. J. Hamer, and J. Oitmaa, J. Phys. A **23**, 1775 (1990).

[9] M. P. Gelfand, R. R. P. Singh, and D. A. Huse, J. Stat. Phys. **59**, 1093 (1990).

[10] T. Barnes, J. Riera, and D. A. Tennant, Phys. Rev. B **59**, 11 384 (1999).

[11] C. Knetter and G. S. Uhrig, Eur. Phys. J. B **13**, 209 (2000).

[12] Z. J. Wegner, Ann. Phys. (Leipzig) **3**, 77 (1994).

[13] Some mixed third order hopping amplitudes in Ref. 3 and Eq. (2) are incorrect: t_0: $+(8\overline{\alpha}-16\overline{\beta}+18\overline{\alpha\beta}+9\overline{\beta^2}-12\overline{\alpha\beta^2})\lambda\mu^2/32$ should be $+(8\overline{\alpha}-16\overline{\beta}+15\overline{\alpha\beta^2})\lambda\mu^2/32$; $+\lambda^4/128$ should be $-\lambda^4/128$; $-3\lambda^2\mu^2/16$ should be $-\lambda^2\mu^2/32$; t_{10}: $+2\overline{\alpha\beta^2}\lambda\mu^2/32$ should be $+\overline{\alpha\beta^2}\lambda\mu^2/64$; $+\lambda^2\mu^2/32$ should be $+3\lambda^2\mu^2/64$; t_{11}: $+7\overline{\alpha^2}\overline{\beta}\lambda^2\mu/128$ should be $+4\overline{\alpha^2}\overline{\beta}\lambda^2\mu/128$; $+7\overline{\beta^3}\mu^3/128$ should be $+4\overline{\beta^3}\mu^3/128$; $+5\lambda^2\mu^2/128$ should be $+9\lambda^2\mu^2/128$; t_{21}: $-5\overline{\alpha^2}\overline{\beta}/\lambda^2\mu/256$ should be $-2\overline{\alpha^2}\overline{\beta}\lambda^2\mu/256$; $-3\overline{\beta^3}\mu^3/256$ should be $-3\overline{\beta^3}\mu^3/128$.

[14] L. P. Regnault, M. Aïn, B. Hennion, G. Dhalenne, and A. Revcolevschi, Phys. Rev. B **53**, 5579 (1996).

[15] H. Rosner and S.-L. Drechsler, Phys. Rev. B (to be published).

[16] M. Braden, G. Wilkendorf, J. Lorenzana, M. Aïn, G. J. McIntyre, M. Behruzi, G. Heger, G. Dhalenne, and A. Revcolevschi, Phys. Rev. B **54**, 1105 (1996).

[17] A. Fledderjohann and C. Gros, Europhys. Lett. **37**, 189 (1997).

[18] J. Riera and A. Dobry, Phys. Rev. B **51**, 16 098 (1995).

[19] G. Castilla, S. Chakravarty, and V. J. Emery, Phys. Rev. Lett. **75**, 1823 (1995).

[20] K. Fabricius, A. Klümper, U. Löw, B. Büchner, T. Lorenz, G. Dhalenne, and A. Revcolevschi, Phys. Rev. B **57**, 1102 (1998).

[21] G. Bouzerar, Ö. Legeza, and T. Ziman, Phys. Rev. B **60**, 15 278 (1999).

[22] A. Bühler, N. Elstner, and G. S. Uhrig, Eur. Phys. J. B **16**, 475 (2000).

[23] A. Bühler, U. Löw, and G. S. Uhrig (unpublished).

[24] M. Honda, T. Shibata, K. Kindo, S. Sugai, T. Takeuchi, and H. Hori, J. Phys. Soc. Jpn. **65**, 691 (1996).

[25] B. Pilawa, J. Phys.: Condens. Matter **9**, 3779 (1997).

[26] R. Werner, C. Gros, and M. Braden, Phys. Rev. B **59**, 14 356 (1999).

[27] G. S. Uhrig, Phys. Rev. B **57**, R14 004 (1998).

[28] G. S. Uhrig and B. Normand, cond-mat/0010168 (unpublished).

[29] J. P. Pouget, L. P. Regnault, M. Aïn, B. Hennion, J. P. Renard, P. Veillet, G. Dhalenne, and A. Revcolevschi, Phys. Rev. Lett. **72**, 4037 (1994).

[30] B. Dumoulin, C. Bourbonnais, S. Ravy, J. P. Pouget, and C. Coulon, Phys. Rev. Lett. **76**, 1360 (1996).

[31] G. Wellein, H. Fehske, and A. P. Kampf, Phys. Rev. Lett. **81**, 3956 (1998).

[32] B. Büchner, H. Fehske, A. P. Kampf, and G. Wellein, Physica B **261**, 956 (1999).

[33] S. Trebst, N. Elstner, and H. Monien, cond-mat/9907266 (unpublished).

[34] R. A. Cowley, B. Lake, and D. A. Tennant, J. Phys.: Condens. Matter **18**, L179 (1996).

[35] W. Brenig, Phys. Rev. B **56**, 14 441 (1997).

[36] W. Geertsma and D. Khomskii, Phys. Rev. B **54**, 3011 (1996).

[37] S. Feldkemper and W. Weber, Phys. Rev. B **62**, 3816 (2000).